

Simple model for the gap in the surface states of the antiferromagnetic topological insulator MnBi_2Te_4

R. S. Akzyanov^{a,b,c,*}, A. L. Rakhmanov^{a,c}

^a*Dukhov Research Institute of Automatics, Sushchevskaya 22 st., 127030, Moscow, Russia*

^b*Moscow Institute of Physics and Technology, Dolgoprudny, Moscow Region, 141700 Russia*

^c*Institute for Theoretical and Applied Electrodynamics, Russian Academy of Sciences, Moscow, 125412 Russia*

Abstract

We study the influence of the antiferromagnetic order on the surface states of topological insulators. We derive an effective Hamiltonian for these states, taking into account the spatial structure of the antiferromagnetic order. We obtain a typical (gapless) Dirac Hamiltonian for the surface states when the surface of the sample is not perturbed. Gapless spectrum is protected by the combination of time-reversal and half-translation symmetries. However, a shift in the chemical potential of the surface layer opens a gap in the spectrum away from the Fermi energy. Such a gap occurs only in systems with finite antiferromagnetic order. We observe that the system topology remains unchanged even for large values of the disorder. We calculate the spectrum using the tight-binding model with different boundary conditions. In this case we get a gap in the spectrum of the surface states. This discrepancy arises due to the violation of the combined time-reversal symmetry. We compare our results with experiments and density functional theory calculations.

Keywords: antiferromagnetic topological insulator; surface states; disorder

1. Introduction

Magnetic topological insulators (MTIs) are narrow-gap semiconductors that exhibit a nontrivial band structure along with magnetic order [1–3]. A prominent feature of the topological insulators (TIs) is the presence of the surface states that are robust against disorder [4, 5]. The exchange interaction in the MTIs breaks the time-reversal symmetry of the system and can open a band gap in the spectrum of the surface electron states [6, 7]. This significantly distinguishes MTIs from non-magnetic TIs and makes it possible to observe the anomalous quantum Hall effect and chiral Majorana states [8, 9].

The magnetic order in the TIs can be introduced either by doping a non-magnetic TI with magnetic atoms or by synthesis of the stoichiometric TI with magnetic ions in its crystal structure. The latter approach looks more promising since it allows to obtain homogeneous samples. The first synthesized intrinsic MTI was MnBi_2Te_4 [10–23], which is currently being intensively studied. This material has a layered Van-der-Waals structure. Each seven-atom block or layer of MnBi_2Te_4 can be schematically written as Te-Bi-Te-Mn-Te-Bi-Te (see Fig. 1). Magnetic ions of Mn are ferromagnetically ordered within the layer, and the layers are ordered antiferromagnetically (AFM). The Neel temperature for MnBi_2Te_4 is 25 K [10, 13], which is the largest among existing MTIs.

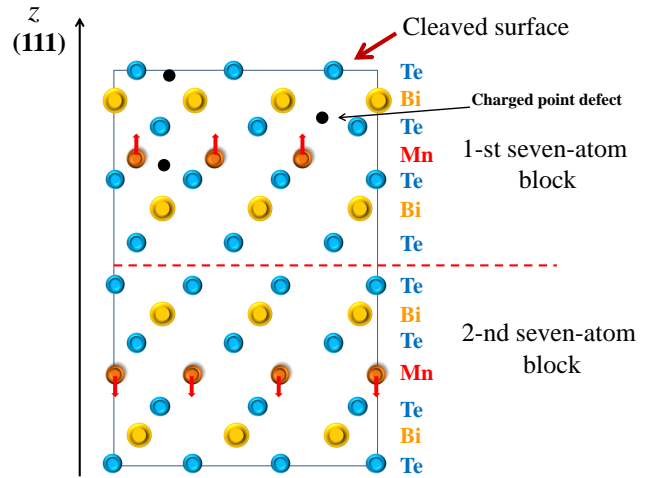


Figure 1: Schematic structure of the antiferromagnetic topological insulator MnBi_2Te_4 . The red up and down arrows on the circles represent spin up and spin down AFM magnetization, the black dots represents charged impurities at the surface layer. Surface orientation corresponds to the (111) crystallographic plane.

In the case of AFM MTIs, it is an open question whether the spectrum of the surface states has a gap or not. Density functional theory (DFT) calculations predict the gap spectrum for the surface states [10, 24, 25]. The ARPES measurements give a wide range of the gap from 0 [17] to 100 meV [26]. Such a scattering of results can be attributed to differences in sample quality. Other explanations include the surface electrostatic field [27], increasing

*Corresponding author.

Email address: akzyanov@phystech.edu (R. S. Akzyanov)

the interlayer distance between the van der Waals block near the surface [28], and native point defects [29]. Thus, the influences of material parameters and defects on the electronic gap in the spectrum of MTIs are important issues. To address these issues, the *ab initio* calculations of the energy spectrum of MnBi_2Te_4 were performed [28] as well as the analytical analysis based on the effective Hamiltonian of the system in the $\mathbf{k} \cdot \mathbf{p}$ approximation [24, 30]. The authors of Ref. [30] obtained an analytical dependence of the surface energy gap on the bulk properties of the MTI. They conclude that a possible reason for the scattering of the experimental data could be attributed to the idea that in real materials the intralayer ferromagnetic order is smaller and more localized than implied by the theoretical analysis. In the seminal paper Ref. [31], based on a toy model for the topological insulator, the authors predicted that the spectrum of surface states in the AFM phase is gapped. Using a different model, the authors obtained that the surface states are detached from the bulk states, implying a rich physics of the surface states in the MTIs in the AFM state depending on the underlying model. In Ref. [32] it was shown that presence of the gap depends on the termination of the surface. All of the above allows us to assert that at present there is no generally accepted understanding of the nature of the gap in the spectrum of surface states in the AFM MTIs.

In Ref. [33] it was observed that the surface doping opens a gap in the spectrum of the surface states. The DFT calculations performed in Refs. [28, 34] predict that the charged impurities at the surface control the surface band gap in MnBi_2Te_4 . Therefore, investigating of the influence of the surface doping on the gap in the surface states is an important task.

In this paper we study the surface states of the AFM MTI. We start with the linearised in momentum MTI Hamiltonian, in which we explicitly consider a spatial variation of the magnetisation across the layers of the material. We then calculate an effective Hamiltonian for the surface states. The Hamiltonian obtained differs from one derived in Ref. [24] since it has an extended basis that includes the indices of the AFM-ordered layers. The effective Hamiltonian for the surface states has a typical Dirac form and the spectrum is gapless. This gapless spectrum is protected by the combined time-reversal symmetry which consists of time-reversal symmetry and half-translation symmetry [24]. However, if we break such a symmetry by perturbing the surface, the gap at the Dirac point appears. We show that the shift of the chemical potential of the surface layer opens a gap in the spectrum at the Dirac point due to the AFM ordering. This gap is robust to disorder, that is, even strong disorder does not suppress the gap to zero. We extend the bulk MTI Hamiltonian to include quadratic out-of-plane momentum terms. We find that such terms violate the combined time-reversal symmetry that allows for a finite gap without surface perturbation. We calculate the spectrum of such a Hamiltonian in a tight-binding approximation and observe a finite gap

for the surface states. We discuss the consistency of our results with the experiment and DFT calculations.

2. Model

We are interested in the electron spectrum of the AFM MTI of the type MnBi_2Te_4 near the Γ -point. Following Ref. [24], we start with a low-energy Hamiltonian in the form

$$H_0 = -\mu + m\sigma_z + v(k_x s_x + k_y s_y)\sigma_x + v_z k_z s_z \sigma_x, \quad (1)$$

where we neglect terms of order k^2 and higher. Here k_i are the components of the momentum \mathbf{k} , v and v_z are the in-plane and transverse components of the Fermi velocity, respectively. The Pauli matrices s_i act in the spin space (\uparrow, \downarrow) and the Pauli matrices σ_i act in the space of the low-energy orbitals ($|P1_z^+\rangle, |P2_z^-\rangle$), where the superscripts \pm stand for the parity of the corresponding states [24]. In the absence of spin-orbit coupling, the states $|P1_z^+ \uparrow(\downarrow)\rangle$ are associated with two Bi orbitals, while $|P2_z^- \uparrow(\downarrow)\rangle$ are associated with two Te orbitals. We will also use more descriptive notations, $\text{Bi}_{\uparrow(\downarrow)}$ and $\text{Te}_{\uparrow(\downarrow)}$, for the low-lying states considered. The spectrum of the Hamiltonian (1) at $k_z = 0$ is $E_0 = -\mu \pm \sqrt{m^2 + v^2 k^2}$, and the physical meaning of m is a gap in the spectrum in the bulk. The Hamiltonian (1) is equivalent to the Hamiltonian for an ordinary TI [6] up to the rotation of the basis.

To describe the magnetic ordering, we should add to H_0 the corresponding magnetic terms. To take into account the spacial structure of the AFM ordering explicitly, one has to consider two seven-atom blocks with Mn atoms having opposite directions of the magnetic moment, which requires extension of the Gilbert space of Hamiltonian (1) from 4D to 8D. However, the authors of Refs. [24, 30] made a projection of the space that neglected this feature. Such an approach allows them to reduce the space of the Hamiltonian from 8D to 4D.

In order to restore information on the spatial structure of the AFM state, we introduce an additional Gilbert space t that takes into account pairs of the magnetic layers with opposite polarization of Mn atoms. In other words, we add additional degree of freedom that can be associated with the even and odd layers in the same way as spin up and spin down regions for the spin degree of freedom. Our approach in this part is similar to the approach from Ref. [31]. First, we transform the kinetic energy term in the Hamiltonian H_0 . This transformation is $v_z k_z s_z \sigma_x \rightarrow v_z k_z s_z \sigma_x t_x$, where t_x is the Pauli matrix that acts in the t space, since only the nearest-neighbour hopping between the Bi and Te orbitals is allowed. In the absence of the AFM order we have half-translational symmetry between even and odd layers $[\hat{H}, \hat{S}] = 0$, where operator of the half-translation is $\hat{S} = t_x$. In general, the AFM ordering results, first, in the finite magnetization M_z of each seven-atom layer and, second, in a spin imbalance between Bi and Te orbitals A_z . Such terms naturally break the symmetry between even

and odd layers. The corresponding term in the Hamiltonian reads

$$H_m = M_z s_z t_z + A_z s_z \sigma_z t_z. \quad (2)$$

This term includes, in particular, the spatial dependence of the magnetization: for even and odd layers we have magnetization with the opposite directions.

Thus, the Hamiltonian of the AFM MTI in the extended space is

$$H = -\mu + m\sigma_z + v(k_x s_x + k_y s_y)\sigma_x + v_z k_z s_z \sigma_x t_x + M_z s_z t_z + A_z s_z \sigma_z t_z. \quad (3)$$

The Pauli matrices $t_i, i = x, y, z$ act in the space of even/odd layers. As we can see, the magnetic terms break the time-reversal symmetry $\hat{T}H(\mathbf{k})\hat{T}^{-1} \neq H(-\mathbf{k})$, where $\hat{T} = i s_y K$ and K is the complex conjugation. The translation symmetry between layers 1 and 2 is also broken by the magnetic terms: $\hat{S}H(\mathbf{k})\hat{S}^{-1} \neq H(\mathbf{k})$, where operator of the half-translation symmetry is $\hat{S} = t_x$. However, a combined time-reversal symmetry $\hat{T}_a H(\mathbf{k})\hat{T}_a^{-1} = H(-\mathbf{k})$ is preserved, where $\hat{T}_a = \hat{S}\hat{T} = i s_y t_x K$ and $\hat{T}_a^2 = -1$. This symmetry ensures Kramer's degeneracy of the spectrum.

3. Surface states

We assume that the sample occupies the space $z > 0$ and its surface lies in the (x, y) plane at $z = 0$ that corresponds to the crystallographic plane (111) of the natural cleavage. We replace k_z by the operator $-i\partial_z$ in the Hamiltonian ($\hbar = 1$) and put $k_x, k_y = 0$ in the main approximation in \mathbf{k} . As a result, the surface states $\Psi(z)$ obey the equation

$$[m\sigma_z + s_z(M_z t_z + A_z \sigma_z t_z - i v_z \sigma_x t_x \partial_z) - \mu]\Psi = E\Psi, \quad (4)$$

where E is the energy. We choose $E = 0$ since we are interested in the states near the Dirac point. We seek the solution to the problem in the form of an eighth-component spinor

$$\Psi = (\text{Bi}_{\uparrow 1}, \text{Bi}_{\downarrow 1}, \text{Te}_{\uparrow 1}, \text{Te}_{\downarrow 1}, \text{Bi}_{\uparrow 2}, \text{Bi}_{\downarrow 2}, \text{Te}_{\uparrow 2}, \text{Te}_{\downarrow 2}). \quad (5)$$

Each component of the spinor is characterised by three quantum numbers: the orbital index $\sigma = \text{Bi}, \text{Te}$, the spin projection $s = \uparrow, \downarrow$ and the magnetic layer number $t = 1, 2$. In addition, the normalisation condition $\int_0^{+\infty} |\Psi(z)|^2 dz = 1$ should be satisfied.

The boundary problem should be accompanied by a proper boundary condition for the wave function. We start with the discussion of non-magnetic TI. A uniform boundary condition $\Psi(0) = 0$ for non-magnetic TI was proposed in Ref. [6]. However, in the linear approximation in ∂_z such a problem has only a trivial solution. In Refs. [35, 36] the authors found that the van der Waals system Bi_2Se_3 is naturally cleaved between two quintuple layer blocks. This allows the formulation of appropriate

boundary conditions. Obviously a similar situation is realised for MnBi_2Te_4 , but now we have the seven layer unit and two AFM ordered blocks. Following the approach of Refs. [35, 36], we express the boundary conditions in our matrix notation in the form

$$(1 + \sigma_x)(1 + t_z)\Psi(0) = 0, \quad \Psi(+\infty) = 0. \quad (6)$$

Physically, this condition implies that only one magnetic layer and only one orbital on a proper basis reach the surface. Such boundary condition preserves time-reversal and C_3 rotational symmetries. Linear equations (4) along with the boundary conditions Eq. (6) and normalization conditions form a complete system of equations that allows us to calculate the spinor Ψ for the surface states. We obtain two linearly independent solutions. It is convenient to introduce an orthonormal basis (Ψ_1, Ψ_2) , and any solution Ψ is a linear combination of Ψ_1 and Ψ_2 . We choose Ψ_1 and Ψ_2 in the form

$$\begin{aligned} \Psi_1 &= \text{Bi}_{\uparrow 1}^{(0)}(e^{\lambda_1 z}, 0, -e^{\lambda_2 z}, 0, -i\kappa_1 e^{\lambda_2 z}, 0, i\nu_2 e^{\lambda_1 z}, 0), \\ \Psi_2 &= \text{Bi}_{\downarrow 1}^{(0)}(0, e^{\lambda_2 z}, 0, -e^{\lambda_1 z}, 0, -i\nu_1 e^{\lambda_1 z}, 0, i\kappa_2 e^{\lambda_2 z}), \end{aligned} \quad (7)$$

where

$$\begin{aligned} \text{Bi}_{\uparrow 1}^{(0)} &= \left[\frac{M_z + m}{|\lambda_1|(M_z + m - A_z + \mu)} + \frac{M_z - m}{|\lambda_2|(M_z - m + A_z + \mu)} \right]^{-\frac{1}{2}}, \\ \text{Bi}_{\downarrow 1}^{(0)} &= \left[\frac{M_z + m}{|\lambda_1|(M_z + m + A_z - \mu)} + \frac{M_z - m}{|\lambda_2|(M_z - m - A_z - \mu)} \right]^{-\frac{1}{2}}, \\ \kappa_{1,2} &= \sqrt{\frac{M_z - m \mp A_z \mp \mu}{M_z - m \pm A_z \pm \mu}}, \quad \nu_{1,2} = \sqrt{\frac{M_z + m \mp A_z \mp \mu}{M_z + m \pm A_z \pm \mu}} \\ \lambda_{1,2} &= -\frac{1}{v_z} \sqrt{(M_z \pm m)^2 - (A_z \mp \mu)^2}. \end{aligned} \quad (8)$$

The surface states exist if $\text{Re}\lambda_i < 0$ for both $i = 1, 2$. This constraint imposes conditions on the values of the parameters under which the surface states can exist. We checked that the current does not flow through the plane.

4. Effective Hamiltonian for the surface states

To derive an effective surface Hamiltonian H_s we make a projection of the Hamiltonian (3) on the basis vectors Eqs. (7), $H_s = \langle \Psi_i | H | \Psi_j \rangle$. After integration over z , and considering $v(k_x s_x + k_y s_y)\sigma_x$ as a perturbation we obtain a typical Dirac-like Hamiltonian for the surface states

$$\begin{aligned} H_s &= \tilde{v}(k_x \hat{s}_x + k_y \hat{s}_y), \\ \tilde{v} &= v \frac{\text{Bi}_{\uparrow 1}^{(0)} \text{Bi}_{\downarrow 1}^{(0)} (|\lambda_1| + |\lambda_2|)}{|\lambda_1 \lambda_2|}, \end{aligned} \quad (9)$$

where \hat{s} are the Pauli matrices in the space of the vectors Ψ_1 and Ψ_2 . The Hamiltonian has a linear gapless spectrum $E = \pm \tilde{v} \sqrt{k_x^2 + k_y^2}$. If we assume that the bulk gap is large,

$m \gg |M_z|, |A_z|$, we derive $\tilde{v} = v(1 - \mu^2/m^2) + O(M_z^2) + O(A_z^2)$.

The wave function Ψ_1 corresponds to the orbitals with the real spin projection $s_z = \uparrow$, while Ψ_2 corresponds to $s_z = \downarrow$, see Eqs. (7). In addition, in our orthonormalized basis $\hat{s}_\alpha \propto \langle \Psi_i | s_\alpha | \Psi_j \rangle$. Therefore, we can consider the Pauli matrices in the space of the surface states \hat{s} as real-spin operators. Note that a similar result for the surface states was obtained in Ref. [6].

We see that the AFM ordering affects only quantitatively the surface states, as compared to the non-magnetic case $M_z = A_z = 0$ [24, 30]. This result is not surprising: in both non-magnetic and AFM cases, the system has the same symmetries except the time-reversal symmetry \hat{T} . However, the AFM TI has emergent time-reversal-like symmetry \hat{T}_a in the extended space, as it was stated in Section 2. Therefore, we need to break symmetry between layers 1 and 2 with different polarizations of Mn atoms to observe a qualitatively new result. The simplest way to break this symmetry is to introduce a difference in the chemical potential between layers 1 and 2 due to surface doping. For simplicity, we assume that the chemical potential in the bulk and in the second seven-atom block is the same, while it is different in the single surface block. We introduce the operator of the surface chemical potential as

$$\hat{\mu}_s = -\mu_s \frac{\hat{1} + t_z}{2}, \quad (10)$$

where factor $(1 + t_z)/2$ selects single seven-atom block 1 as the surface termination and μ_s is a difference between chemical potentials in the layers 1 and 2. Now we calculate matrix elements $\hat{\mu}_{ij} = \langle \Psi_i | \hat{\mu}_s | \Psi_j \rangle$ that gives us

$$\begin{aligned} \hat{\mu} &= -\tilde{\mu}_s(1 + \delta \hat{s}_z), \\ \tilde{\mu}_s &= \mu_s \frac{(\text{Bi}_{\uparrow 1}^{(0)2} + \text{Bi}_{\downarrow 1}^{(0)2}) (|\lambda_1| + |\lambda_2|)}{2\sqrt{2}|\lambda_1 \lambda_2|}, \\ \delta &= \frac{\text{Bi}_{\uparrow 1}^{(0)2} - \text{Bi}_{\downarrow 1}^{(0)2}}{\text{Bi}_{\uparrow 1}^{(0)2} + \text{Bi}_{\downarrow 1}^{(0)2}}. \end{aligned} \quad (11)$$

When $m \gg |M_z|, |A_z|$ we get $\delta = M_z \mu / m^2 (1 + \mu^2 / 2m^2) + A_z / m (1/2 + \mu^2 / m^2)$. We can see that the shift of the surface chemical potential brings the term $\propto \hat{s}_z$ that opens a gap in the spectrum of the surface states of the MTI. The effective Hamiltonian (9) with the surface perturbation now reads as

$$H = \tilde{v}(k_x \hat{s}_x + k_y \hat{s}_y) - \tilde{\mu}_s(1 + \delta \hat{s}_z). \quad (12)$$

The spectrum of this Hamiltonian is

$$E_{\pm} = -\tilde{\mu}_s \pm \sqrt{\tilde{v}^2 k^2 + \tilde{\mu}_s^2 \delta^2}. \quad (13)$$

The finite δ induces a gap between E_+ and E_- . This term arises due to the finite charge imbalance between the top layer and the next layer, given by the t_z term in Eq. 10.

We plot in Fig. 2 (right panel) the parameter δ that controls the gap in the surface spectrum as a function of

the AFM magnetization M_z for different values of the bulk chemical potential μ and A_z . We see that $\delta \propto M_z$, μ controls the slope of this line, and A_z shifts $\delta(M_z)$ from the coordinate origin. The larger are μ and M_z , the larger is the surface electron gap. The spectrum $E(\mathbf{k})$, Eq. (13), is shown in Fig. 2 (left panel) for different values of $\tilde{\mu}_s$. When we ignore the AFM order, $M_z = A_z = 0$, the gap vanishes since $\delta = 0$ in this case.

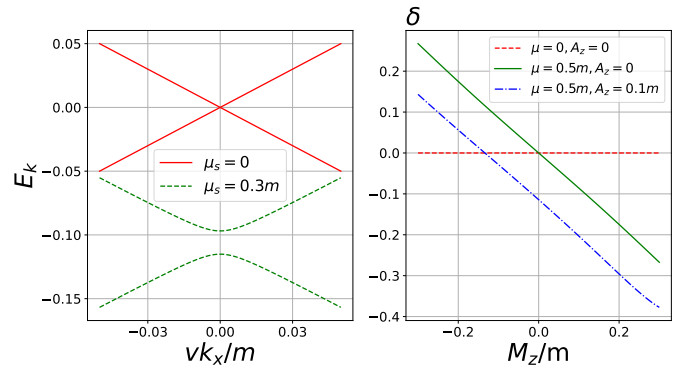


Figure 2: Left panel: energy spectrum as a function of the momentum k_x and $k_y = 0$. We take $\mu = 0.5m$, $M_z = 0.1m$, $A_z = 0$. Spectrum have a gap if $\mu_s \neq 0$. Right panel: parameter δ as a function of the AFM magnetization M_z .

5. Tight-binding model with the quadratic terms

In this section we numerically study the energy spectrum of the tight-binding model based on the Hamiltonian (1) with the AFM terms given by Eq. (2). We also extend the model to include the quadratic terms in the momentum. Following Ref. [24] we replace $\mu \rightarrow \mu + C_1 k_z^2 + C_2(k_x^2 + k_y^2)$ and $m \rightarrow m + M_1 k_z^2 + M_2(k_x^2 + k_y^2)$. The quadratic terms in k_z double the order of the differential equations (4). In this case the boundary conditions given by Eq. (6) are no longer sufficient. Instead we use the following boundary conditions [6, 24]

$$(1 + t_z)\Psi(0) = 0, \quad \Psi(+\infty) = 0, \quad (14)$$

assuming that the wave function Ψ vanishes at the surface and in the bulk. We map the low-energy Hamiltonian to the tight-binding model and numerically calculate the electron spectrum of the surface states. The result is shown in Fig. 3. We see that the finite AFM order opens a gap in the spectrum of the surface states. This result is in agreement with the tight-binding calculations made in [28, 34].

To get an idea of the appearance of the gap when we consider quadratic momentum, we explain in detail in Appendix A how we extend the model basis to include the degrees of freedom associated with the layers having opposite magnetic momenta. We find that the low energy Hamiltonian is written now as

$$H_2 = H + C_1 k_z^2 t_x + C_1 k_z t_y / a + M_1 k_z^2 \sigma_z t_x + M_1 k_z \sigma_z t_y / a,$$

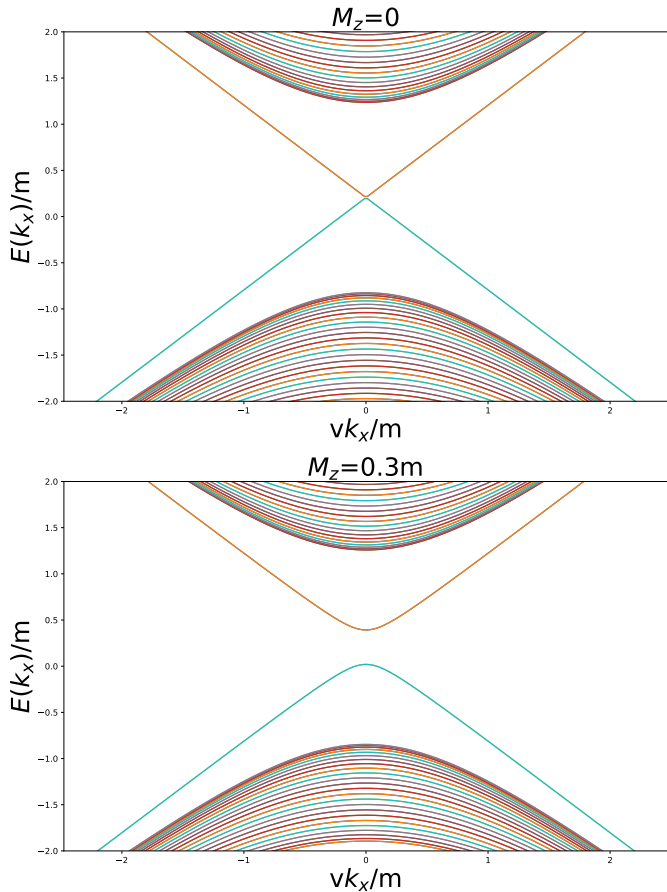


Figure 3: The spectrum $E(k_x)$ of the tight-binding Hamiltonian for $k_y = 0$ as a function of the in-plane momentum $vk_x/|m|$. Upper figure corresponds to $M_z = A_z = 0$. Lower figure corresponds to $M_z = 0.3m, A_z = 0$. Following Ref. [24] we take $m = -0.12eV$, $\mu = -0.2m$, $v = 3.2eV \cdot \text{\AA}$, $v_z = 2.7eV \cdot \text{\AA}$, $C_1 = 2.7eV \cdot \text{\AA}^2$, $C_2 = 17eV \cdot \text{\AA}^2$, $M_1 = 12eV \cdot \text{\AA}^2$, $M_2 = 9.4eV \cdot \text{\AA}^2$. Also, we set $\mu = -0.2m$ and lattice constant $a = 15\text{\AA}$ [37] in order to get gapless surface states without magnetization. The calculations are performed for 200 layers.

where H is given by Eq. (3).

We see that we have terms in both t_x and t_y . If we include only the linear term in k_z in the Hamiltonian (A.1) and exclude the quadratic corrections to the Hamiltonian $C_1 = M_1 = 0$, we have only the t_x part. This case is realised in the Hamiltonian (3). The quadratic in k_z terms give rise to t_y terms in the Hamiltonian, which preserve the time-reversal symmetry \hat{T} but violate the half-translation symmetry $[\hat{S}, t_y] = [t_x, t_y] \neq 0$. This violates the extended time reversal symmetry $\hat{T}_a = \hat{T}\hat{S}$, which leads to the finite gap observed in the calculations.

6. Discussion

In this work we investigate the effects of the antiferromagnetic ordering on the properties of the surface states in the topological insulator. We get that the change in chemical potential at the surface layer opens a gap in the spectrum away from the Fermi energy due to the finite

AFM order. Such a gap is controlled by the value of the surface doping. The gap is robust against disorder. These results are consistent with the experiments that demonstrate opening the surface gap by the surface doping [33]. We should note that in a real samples the effect of the surface defects can be more significant than just electron density disorder and can lead to a quite complex picture [38].

In non-magnetic topological insulators the gapless Dirac spectrum of the surface states is protected by the time-reversal symmetry \hat{T} . Antiferromagnetic order parameter breaks both time-reversal symmetry and symmetry between even and odd layers. Instead, a combined time-reversal-like symmetry $\hat{T}_a = \hat{t}_x\hat{T}$ is preserved. The latter symmetry includes translation between spin-up and spin-down AFM layers [24]. Such a symmetry protects gapless spectrum of the surface states. In order to open a gap in the spectrum this symmetry has to be broken. Since the combined symmetry consist of time-reversal symmetry and translational symmetry we can break any of them. We can violate time-reversal symmetry by the out-of-plane magnetization and open the gap in the similar manner to the topological insulators without the AFM order. The other way is to break symmetry between spin-up and spin-down layers. Unlike real time-reversal symmetry, this combined symmetry can be broken by a non-magnetic perturbation (see, e.g., Eq.(9) to check that $[\hat{T}_a, \hat{\mu}] \neq 0$). If the perturbation breaks symmetry between spin-up and spin-down regions, then, a gap in the spectrum of the surface states can be formed, see Fig. 2. Such mechanism opens a gap in the spectrum only if AFM order is present in the system.

Experimentally, surface disorder is caused by natural exposure of the surface to the atmosphere [39] or by external doping of the surface [33]. Recent DFT calculations of the properties of MnBi_2Te_4 show that doping the first surface layer with Ge increases the gap in the surface states [40]. Also, DFT calculations performed in Ref. [34] show that the surface potential opens a gap in the surface states in the AFM MTI. Experimentally, Sb doping of the surface of MnBi_2Te_4 opens a gap in the spectrum of surface states [33]. We have considered the shift of the surface chemical potential due to an effective surface doping, neglecting the possible disorder of such a perturbation. Therefore, an important question is the stability of the surface gap against disorder. Note that in the case of a magnetisation-induced gap in the surface states of non-magnetic TI, the strong disorder suppresses the gap [41]. In Appendix. B we have shown that the gap in the spectrum of surface states given by Eq. (12) remains finite even for large values of disorder.

The results of the DFT calculations presented in Refs. [10, 24, 25] predict a gap in the spectrum of surface states of the AFM MTI without any surface disorder. These results are consistent with our tight-binding calculations in Sec. 5. The reason for the gap opening is the violation of the combined time-reversal symmetry, which is possible due to different boundary conditions. Further studies are needed to determine which model better describes the

experimental results.

7. Conclusions

In this paper we have derived the Hamiltonian of the bulk states of the magnetic topological insulator which includes the antiferromagnetic order parameter. For this Hamiltonian, we obtain the effective Hamiltonian of the surface states, which has the same form as for the non-magnetic topological insulator. The surface doping opens a gap in the spectrum of surface states due to the finite antiferromagnetic order. We perform tight-binding calculations for different boundary conditions and obtain the gapped spectrum for the surface states.

Declaration of competing interest

The authors declare that they have no known competing financial interests or personal relationships that could have appeared to influence the work reported in this paper.

Acknowledgments

This work is supported by Russian Science Foundation (project № 22-72-10074).

References

- [1] Y. Tokura, K. Yasuda, A. Tsukazaki, Magnetic topological insulators, *Nature Reviews Physics* 1 (2) (2019) 126–143. doi:10.1038/s42254-018-0011-5. URL <https://doi.org/10.1038/s42254-018-0011-5>
- [2] P. Wang, J. Ge, J. Li, Y. Liu, Y. Xu, J. Wang, Intrinsic magnetic topological insulators, *The Innovation* 2 (2) (2021). doi:10.1016/j.xinn.2021.100098. URL <https://doi.org/10.1016/j.xinn.2021.100098>
- [3] B. A. Bernevig, C. Felser, H. Beidenkopf, Progress and prospects in magnetic topological materials, *Nature* 603 (7899) (2022) 41–51. doi:10.1038/s41586-021-04105-x. URL <https://doi.org/10.1038/s41586-021-04105-x>
- [4] M. Z. Hasan, C. L. Kane, Colloquium: Topological insulators, *Rev. Mod. Phys.* 82 (2010) 3045–3067. doi:10.1103/RevModPhys.82.3045. URL <https://link.aps.org/doi/10.1103/RevModPhys.82.3045>
- [5] G. A. Fiete, V. Chua, M. Kargarian, R. Lundgren, A. Rüegg, J. Wen, V. Zyuzin, Topological insulators and quantum spin liquids, *Physica E: Low-dimensional Systems and Nanostructures* 44 (5) (2012) 845–859, sI:Topological Insulators. doi:<https://doi.org/10.1016/j.physe.2011.11.011>. URL <https://www.sciencedirect.com/science/article/pii/S1386947711004061>
- [6] C.-X. Liu, X.-L. Qi, H. Zhang, X. Dai, Z. Fang, S.-C. Zhang, Model hamiltonian for topological insulators, *Phys. Rev. B* 82 (2010) 045122. doi:10.1103/PhysRevB.82.045122. URL <https://link.aps.org/doi/10.1103/PhysRevB.82.045122>
- [7] C.-Z. Chang, C.-X. Liu, A. H. MacDonald, Colloquium: Quantum anomalous hall effect, *Rev. Mod. Phys.* 95 (2023) 011002. doi:10.1103/RevModPhys.95.011002. URL <https://link.aps.org/doi/10.1103/RevModPhys.95.011002>
- [8] K. He, MnBi₂Te₄-family intrinsic magnetic topological materials, *npj Quantum Materials* 5 (1) (2020) 90. doi:10.1038/s41535-020-00291-5. URL <https://doi.org/10.1038/s41535-020-00291-5>
- [9] S. Li, T. Liu, C. Liu, Y. Wang, H.-Z. Lu, X. C. Xie, Progress on antiferromagnetic topological insulator MnBi₂Te₄, *National Science Review* (2023) nwac296arXiv:<https://academic.oup.com/nsr/advance-article-pdf/doi/10.1093/nsr/nwac296/48483824/nwac296.pdf>, doi:10.1093/nsr/nwac296. URL <https://doi.org/10.1093/nsr/nwac296>
- [10] M. M. Otrokov, I. I. Klimovskikh, H. Bentmann, D. Estyunin, A. Zeugner, Z. S. Aliev, S. Gaß, A. Wolter, A. Koroleva, A. M. Shikin, et al., Prediction and observation of an antiferromagnetic topological insulator, *Nature* 576 (7787) (2019) 416–422.
- [11] D. Zhang, M. Shi, T. Zhu, D. Xing, H. Zhang, J. Wang, Topological axion states in the magnetic insulator mnbi 2 te 4 with the quantized magnetoelectric effect, *Physical review letters* 122 (20) (2019) 206401.
- [12] Y. Gong, J. Guo, J. Li, K. Zhu, M. Liao, X. Liu, Q. Zhang, L. Gu, L. Tang, X. Feng, et al., Experimental realization of an intrinsic magnetic topological insulator, *Chinese Physics Letters* 36 (7) (2019) 076801.
- [13] S. H. Lee, Y. Zhu, Y. Wang, L. Miao, T. Pillsbury, H. Yi, S. Kempinger, J. Hu, C. A. Heikes, P. Quarterman, W. Ratcliff, J. A. Borchers, H. Zhang, X. Ke, D. Graf, N. Alem, C.-Z. Chang, N. Samarth, Z. Mao, Spin scattering and noncollinear spin structure-induced intrinsic anomalous hall effect in antiferromagnetic topological insulator MnBi₂Te₄, *Phys. Rev. Res.* 1 (2019) 012011. doi:10.1103/PhysRevResearch.1.012011. URL <https://link.aps.org/doi/10.1103/PhysRevResearch.1.012011>
- [14] Z. S. Aliev, I. R. Amiraslanov, D. I. Nasonova, A. V. Shevelkov, N. A. Abdullayev, Z. A. Jahangirli, E. N. Orujlu, M. M. Otrokov, N. T. Mamedov, M. B. Babanly, et al., Novel ternary layered manganese bismuth tellurides of the mn₂te₃ system: Synthesis and crystal structure, *Journal of Alloys and Compounds* 789 (2019) 443–450.
- [15] Y.-J. Hao, P. Liu, Y. Feng, X.-M. Ma, E. F. Schwier, M. Arita, S. Kumar, C. Hu, M. Zeng, Y. Wang, et al., Gapless surface dirac cone in antiferromagnetic topological insulator mnbi 2 te 4, *Physical Review X* 9 (4) (2019) 041038.
- [16] Y. Chen, L. Xu, J. Li, Y. Li, H. Wang, C. Zhang, H. Li, Y. Wu, A. Liang, C. Chen, et al., Topological electronic structure and its temperature evolution in antiferromagnetic topological insulator mnbi 2 te 4, *Physical Review X* 9 (4) (2019) 041040.
- [17] P. Swatek, Y. Wu, L.-L. Wang, K. Lee, B. Schrunck, J. Yan, A. Kaminski, Gapless dirac surface states in the antiferromagnetic topological insulator mnbi 2 te 4, *Physical Review B* 101 (16) (2020) 161109.
- [18] A. Liang, C. Chen, H. Zheng, W. Xia, K. Huang, L. Wei, H. Yang, Y. Chen, X. Zhang, X. Xu, M. Wang, Y. Guo, L. Yang, Z. Liu, Y. Chen, Approaching a minimal topological electronic structure in antiferromagnetic topological insulator mnbi₂te₄ via surface modification, *Nano Lett.* 22 (11) (2022) 4307–4314. doi:10.1021/acs.nanolett.1c04930. URL <https://doi.org/10.1021/acs.nanolett.1c04930>
- [19] J.-X. Qiu, C. Tzschaschel, J. Ahn, A. Gao, H. Li, X.-Y. Zhang, B. Ghosh, C. Hu, Y.-X. Wang, Y.-F. Liu, D. Bérubé, T. Dinh, Z. Gong, S.-W. Lien, S.-C. Ho, B. Singh, K. Watanabe, T. Taniguchi, D. C. Bell, H.-Z. Lu, A. Bansil, H. Lin, T.-R. Chang, B. B. Zhou, Q. Ma, A. Vishwanath, N. Ni, S.-Y. Xu, Axion optical induction of antiferromagnetic order, *Nature Materials* 22 (5) (2023) 583–590. doi:10.1038/s41563-023-01493-5. URL <https://doi.org/10.1038/s41563-023-01493-5>
- [20] A. Gao, Y.-F. Liu, J.-X. Qiu, B. Ghosh, T. V. Trevisan, Y. Onishi, C. Hu, T. Qian, H.-J. Tien, S.-W. Chen, M. Huang, D. Bérubé, H. Li, C. Tzschaschel, T. Dinh, Z. Sun, S.-C. Ho, S.-W. Lien, B. Singh, K. Watanabe, T. Taniguchi, D. C. Bell, H. Lin, T.-R. Chang, C. R. Du, A. Bansil, L. Fu, N. Ni, P. P. Orth, Q. Ma, S.-Y. Xu, Quantum metric nonlinear hall effect in a topological antiferromagnetic heterostructure, *Science*

- 381 (6654) (2023) 181–186. doi:10.1126/science.adf1506.
URL <https://doi.org/10.1126/science.adf1506>
- [21] N. Wang, D. Kaplan, Z. Zhang, T. Holder, N. Cao, A. Wang, X. Zhou, F. Zhou, Z. Jiang, C. Zhang, S. Ru, H. Cai, K. Watanabe, T. Taniguchi, B. Yan, W. Gao, Quantum-metric-induced nonlinear transport in a topological antiferromagnet, *Nature* (2023). doi:10.1038/s41586-023-06363-3.
URL <https://doi.org/10.1038/s41586-023-06363-3>
- [22] P. Chen, Q. Yao, J. Xu, Q. Sun, A. J. Grutter, P. Quarterman, P. P. Balakrishnan, C. J. Kinane, A. J. Caruana, S. Langridge, A. Li, B. Achinuq, E. Heppell, Y. Ji, S. Liu, B. Cui, J. Liu, P. Huang, Z. Liu, G. Yu, F. Xiu, T. Hesjedal, J. Zou, X. Han, H. Zhang, Y. Yang, X. Kou, Tailoring the magnetic exchange interaction in mnbi2te4 superlattices via the intercalation of ferromagnetic layers, *Nature Electronics* 6 (1) (2023) 18–27. doi:10.1038/s41928-022-00880-1.
URL <https://doi.org/10.1038/s41928-022-00880-1>
- [23] T. Cao, D.-F. Shao, K. Huang, G. Gurung, E. Y. Tsymbal, Switchable anomalous hall effects in polar-stacked 2d antiferromagnet mnbi2te4, *Nano Lett.* 23 (9) (2023) 3781–3787. doi:10.1021/acs.nanolett.3c00047.
URL <https://doi.org/10.1021/acs.nanolett.3c00047>
- [24] D. Zhang, M. Shi, T. Zhu, D. Xing, H. Zhang, J. Wang, Topological axion states in the magnetic insulator mnbi2te4 with the quantized magnetoelectric effect, *Phys. Rev. Lett.* 122 (2019) 206401. doi:10.1103/PhysRevLett.122.206401.
URL <https://link.aps.org/doi/10.1103/PhysRevLett.122.206401>
- [25] J. Li, Y. Li, S. Du, Z. Wang, B.-L. Gu, S.-C. Zhang, K. He, W. Duan, Y. Xu, Intrinsic magnetic topological insulators in van der waals layered mnbi2te4-family materials, *Science Advances* 5 (6) (2019) eaaw5685. arXiv: <https://www.science.org/doi/pdf/10.1126/sciadv.aaw5685>, doi:10.1126/sciadv.aaw5685.
URL <https://www.science.org/doi/abs/10.1126/sciadv.aaw5685>
- [26] A. Zeugner, F. Nietschke, A. U. Wolter, S. Gaß, R. C. Vidal, T. R. Peixoto, D. Pohl, C. Damm, A. Lubk, R. Hentrich, et al., Chemical aspects of the candidate antiferromagnetic topological insulator mnbi2te4, *Chemistry of Materials* 31 (8) (2019) 2795–2806.
- [27] A. M. Shikin, D. Estyunin, N. L. Zaitsev, D. Glazkova, I. I. Klimovskikh, S. Filnov, A. G. Rybkin, E. Schvier, S. Kumar, A. Kimura, et al., Sample-dependent dirac-point gap in mnbi 2 to 4 and its response to applied surface charge: A combined photoemission and ab initio study, *Physical Review B* 104 (11) (2021) 115168.
- [28] A. M. Shikin, D. Estyunin, I. I. Klimovskikh, S. Filnov, E. Schvier, S. Kumar, K. Miyamoto, T. Okuda, A. Kimura, K. Kuroda, et al., Nature of the dirac gap modulation and surface magnetic interaction in axion antiferromagnetic topological insulator mnbi 2 te 4, *Scientific Reports* 10 (1) (2020) 13226.
- [29] M. Garnica, M. M. Otrokov, P. C. Aguilar, I. I. Klimovskikh, D. Estyunin, Z. S. Aliev, I. R. Amiraslanov, N. A. Abdullayev, V. N. Zverev, M. B. Babanly, et al., Native point defects and their implications for the dirac point gap at mnbi2te4 (0001), *npj Quantum Materials* 7 (1) (2022) 7.
- [30] H.-P. Sun, C. Wang, S.-B. Zhang, R. Chen, Y. Zhao, C. Liu, Q. Liu, C. Chen, H.-Z. Lu, X. Xie, Analytical solution for the surface states of the antiferromagnetic topological insulator mnbi 2 te 4, *Physical Review B* 102 (24) (2020) 241406.
- [31] R. S. Mong, A. M. Essin, J. E. Moore, Antiferromagnetic topological insulators, *Physical Review B* 81 (24) (2010) 245209.
- [32] R. C. Walko, T. Zhu, A. J. Bishop, R. K. Kawakami, J. A. Gupta, Scanning tunneling microscopy study of the antiferromagnetic topological insulator mnbi2se4, *Physica E: Low-dimensional Systems and Nanostructures* 143 (2022) 115391. doi:<https://doi.org/10.1016/j.physe.2022.115391>.
URL <https://www.sciencedirect.com/science/article/pii/S1386947722002272>
- [33] X.-M. Ma, Y. Zhao, K. Zhang, S. Kumar, R. Lu, J. Li, Q. Yao, J. Shao, F. Hou, X. Wu, M. Zeng, Y.-J. Hao, Z. Hao, Y. Wang, X.-R. Liu, H. Shen, H. Sun, J. Mei, K. Miyamoto, T. Okuda, M. Arita, E. F. Schvier, K. Shimada, K. Deng, C. Liu, J. Lin, Y. Zhao, C. Chen, Q. Liu, C. Liu, Realization of a tunable surface dirac gap in sb-doped mnbi2te4, *Phys. Rev. B* 103 (2021) L121112. doi:10.1103/PhysRevB.103.L121112.
URL <https://link.aps.org/doi/10.1103/PhysRevB.103.L121112>
- [34] A. Shikin, D. Estyunin, D. Glazkova, S. Fil’nov, I. Klimovskikh, Electronic and spin structures of intrinsic antiferromagnetic topological insulators of the mnbi2te4 (bi2te3) m family and their magnetic properties (brief review), *JETP Letters* 115 (4) (2022) 213–225.
- [35] L. Fu, E. Berg, Odd-parity topological superconductors: Theory and application to cu_xbi₂se₃, *Phys. Rev. Lett.* 105 (2010) 097001. doi:10.1103/PhysRevLett.105.097001.
URL <https://link.aps.org/doi/10.1103/PhysRevLett.105.097001>
- [36] T. H. Hsieh, L. Fu, Majorana fermions and exotic surface andreev bound states in topological superconductors: Application to cu_xbi₂se₃, *Phys. Rev. Lett.* 108 (2012) 107005. doi:10.1103/PhysRevLett.108.107005.
URL <https://link.aps.org/doi/10.1103/PhysRevLett.108.107005>
- [37] J.-Q. Yan, Q. Zhang, T. Heitmann, Z. Huang, K. Y. Chen, J.-G. Cheng, W. Wu, D. Vaknin, B. C. Sales, R. J. McQueeney, Crystal growth and magnetic structure of mnbi2te4, *Phys. Rev. Mater.* 3 (2019) 064202. doi:10.1103/PhysRevMaterials.3.064202.
URL <https://link.aps.org/doi/10.1103/PhysRevMaterials.3.064202>
- [38] H. Tan, B. Yan, Distinct magnetic gaps between antiferromagnetic and ferromagnetic orders driven by surface defects in the topological magnet mnbi2te4, *Phys. Rev. Lett.* 130 (2023) 126702. doi:10.1103/PhysRevLett.130.126702.
URL <https://link.aps.org/doi/10.1103/PhysRevLett.130.126702>
- [39] M. Brahlek, Y. S. Kim, N. Bansal, E. Edrey, S. Oh, Surface versus bulk state in topological insulator Bi2Se3 under environmental disorder, *Applied Physics Letters* 99 (1) (2011) 012109. arXiv:<https://pubs.aip.org/aip/apl/article-pdf/doi/10.1063/1.3607484/14452748/012109\1\online.pdf>, doi:10.1063/1.3607484.
URL <https://doi.org/10.1063/1.3607484>
- [40] T. P. Estyunina, A. M. Shikin, D. A. Estyunin, A. V. Eryzhenkov, I. I. Klimovskikh, K. A. Bokai, V. A. Golyashov, K. A. Kokh, O. E. Tereshchenko, S. Kumar, K. Shimada, A. V. Tarasov, Evolution of mn1-xgexbi2te4 electronic structure under variation of ge content, *Nanomaterials* 13 (14) (2023). doi:10.3390/nano13142151.
URL <https://www.mdpi.com/2079-4991/13/14/2151>
- [41] R. S. Akzyanov, Born approximation study of the strong disorder in magnetized surface states of a topological insulator, *Phys. Rev. B* 107 (2023) 205416. doi:10.1103/PhysRevB.107.205416.
URL <https://link.aps.org/doi/10.1103/PhysRevB.107.205416>

Appendix A. Derivation of the low energy Hamiltonian in an extended space with quadratic terms

We start with the low energy Hamiltonian, which is presented in a general form

$$H_g = H_0 + \alpha_0 k_z + \beta_0 k_z^2, \quad (\text{A.1})$$

where H_0 , α , β are some hermitian matrices. Here we do a substitution $k_z a \rightarrow \sin k_z a$ and $(k_z a)^2 \rightarrow 2(1 - \cos k_z a)$,

where a is the lattice constant, and get

$$H_g = H + \alpha \sin k_z a + \beta \cos k_z a. \quad (\text{A.2})$$

Here $H = H_0 + 2\beta_0/a^2$, $\alpha = \alpha_0/a$, $\beta = -2\beta_0/a^2$. This Hamiltonian corresponds to the following tight-binding model in real space

$$H_{tb} = h_0 + h_1 + h_2 \quad (\text{A.3})$$

$$h_0 = \sum_n a_n^\dagger H a_n + h.c. \quad (\text{A.4})$$

$$h_1 = \sum_n (a_{n+1}^\dagger \alpha a_n - h.c.)/2i, \quad (\text{A.5})$$

$$h_2 = \sum_n (a_{n+1}^\dagger \beta a_n + h.c.)/2, \quad (\text{A.6})$$

where a_n is the annihilation operator of the electron in the layer n . We introduce new annihilation operators for odd and even layers $c_n = a_{2n+1}$, $d_n = a_{2n}$. We focus only on the terms h_1 and h_2 , since h_0 is trivially transformed:

$$h_1 = \sum_n (c_{n+1}^\dagger \alpha d_n + d_n^\dagger \alpha c_n - h.c.)/2i, \quad (\text{A.7})$$

$$h_2 = \sum_n (c_{n+1}^\dagger \beta d_n + d_n^\dagger \beta c_n + h.c.)/2. \quad (\text{A.8})$$

We perform a Fourier transform on the operators $c_k = \sum_n c_n \exp(-2ik_z n a)$ and $d_k = \sum_n d_n \exp(-2ik_z n a)$, taking into account that the length of the elementary lattice is doubled when we introduce even and odd layers. After that we have

$$h_1 = (c_k^\dagger \alpha d_k e^{2ik_z a} + d_k^\dagger \alpha c_k - h.c.)/2i, \quad (\text{A.9})$$

$$h_2 = (c_k^\dagger \beta d_k e^{2ik_z a} + d_k^\dagger \beta c_k + h.c.)/2. \quad (\text{A.10})$$

We can rewrite the result in the matrix form

$$h_{1,2} = (c^\dagger \ d^\dagger) H_{1,2} \begin{pmatrix} c \\ d \end{pmatrix} \quad (\text{A.11})$$

where

$$H_1 = \frac{\alpha}{2} \begin{pmatrix} 0 & \sin 2k_z a - i(1 - \cos 2k_z a) \\ \sin 2k_z a + i(1 - \cos 2k_z a) & 0 \end{pmatrix} \quad (\text{A.12})$$

and

$$H_2 = \frac{\beta}{2} \begin{pmatrix} 0 & 1 + \cos 2k_z a + i \sin 2k_z a \\ 1 + \cos 2k_z a - i \sin 2k_z a & 0 \end{pmatrix} \quad (\text{A.13})$$

We introduce Pauli matrices t_i , $i = 0, x, y, z$ acting in the odd/even layer space (c, d) . We extend the sine and cosine terms up to $O(k_z^3)$ and obtain a low energy Hamiltonian in the extended space

$$H_{ge} = H_0 + \alpha_0 k_z (t_x + t_y k_z a) + 2\beta_0 k_z (t_x k_z + t_y/a). \quad (\text{A.14})$$

Appendix B. Effects of the disorder

We consider a short-range disorder near the sample surface of the AFM MTI produced by randomly distributed charged point defects, see Fig. 1. Such a perturbation can be more intensive in the surface layer 1 since it is naturally least protected from external influences. We denote 2D density of the point defects as n and the local impurity potential at the position $\mathbf{r} = \mathbf{R}_j$ as u_j . By analogy with Eq. (11), the operator of the disorder potential in the basis of the surface states has a form $\hat{U} = \sum_j \hat{U}_j$, where $\hat{U}_j(\mathbf{r}) = (\hat{1} + \delta t_z) u_j \delta(\mathbf{r} - \mathbf{R}_j)/2$ and $\delta(\mathbf{r})$ is the delta function. We assume that the disorder is Gaussian, that is, $\langle \hat{U}_j(\mathbf{r}) \rangle = 0$ and $\langle \hat{U}_i(\mathbf{r}_1) \hat{U}_j(\mathbf{r}_2) \rangle = n u_0^2 \delta(\mathbf{r}_1 - \mathbf{r}_2) \delta_{ij}$, where $\langle \dots \rangle$ means the spatial average, $u_0^2 = \langle u_i^2 \rangle$, and δ_{ij} is the Kronecker symbol.

We assume that the disorder is weak, that is, $j = n u_0^2 / (2\pi \tilde{v}^2) < 1$ and, following a standard procedure, calculate the self-energy $\hat{\Sigma}$ in the Born approximation. As a result, we obtain in the n -th order a recursive Born series

$$\begin{cases} \hat{\Sigma}^{(n+1)} = \sum_{k,i} \langle \hat{U}_i G(\hat{\Sigma}^{(n)}) \hat{U}_i \rangle, \\ G^{-1}(\hat{\Sigma}^{(n)}) = -H - \hat{\Sigma}^{(n)}. \end{cases} \quad (\text{A.1})$$

If this procedure converges and $\hat{\Sigma}^{(n)} \rightarrow \hat{\Sigma}$ for $n \rightarrow +\infty$, then, the sum of the series can be represented as a self-consistent Born approximation (SCBA) solution: $\hat{\Sigma} = \sum_i \langle \hat{U}_i G(\hat{\Sigma}) \hat{U}_i \rangle$.

We obtain that in the AFM MTI, the self-energy of the disorder has a non-trivial spin structure $\hat{\Sigma} = \Sigma_0 + \Sigma_z s_z$. We perform a transformation $\Sigma_0 = g_0 + \delta g_z$, $\Sigma_z = \delta g_0 + g_z$, and after integration over momentum and summation over i derive from Eqs. (A.1)

$$g_0^{(n+1)} = j(1 - \delta^2) \frac{\tilde{\mu}_s - g_0^{(n)}}{2} \Xi^{(n)}, \quad (\text{A.2})$$

$$g_z^{(n+1)} = \frac{1}{2} j(1 - \delta^2) g_z^{(n)} \Xi^{(n)},$$

$$\Xi^{(n)} = \ln \frac{\tilde{v}^2 k_c^2}{(\delta^2 - 1) \left[\left(\tilde{\mu}_s - g_0^{(n)} \right)^2 - g_z^{2(n)} \right]},$$

where k_c is a cut-off momentum. The obtained result is equivalent to the self-energy equations for the Dirac Hamiltonian without magnetization [41]. Following Ref. [41], we take $g_0^{(0)} = -i0$ and $g_z^{(0)} = 0$, which implies that $g_z^{(n)} = 0$ and $\Sigma_z^{(n)} = \delta \Sigma_0^{(n)}$. We plot self-energy components in Fig. B.4. We see that the disorder generates a real part of the self-energy. The main effect of the disorder is the increase of the surface chemical potential $\tilde{\mu}_s \rightarrow \tilde{\mu}_s - \text{Re} \Sigma_0$, which gives rise to the increase of the gap $\delta \tilde{\mu}_s$.

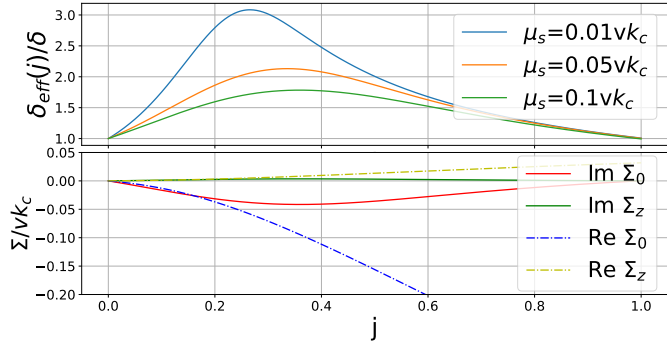


Figure B.4: Upper figure: the value of the renormalized gap $\delta_{\text{eff}} = \delta(\mu_s - \text{Re } \Sigma_0)/\delta\mu_s$ as a function of the disorder strength j for different values of the surface chemical potential μ_s . Lower figure: the self-energy components as a function of the disorder strength j for $\mu_s = 0.1vk_c$. We take $n = 5000$, $\mu = 0.5m$, $M_z = 0.1m$, $A_z = 0$ for both figures.